

performance has been really enhanced, as  $W_1$  is widened from 0.6 to 1.2 mm.

#### 4. CONCLUSION

In this work, a novel periodic electromagnetic bandgap structure has been presented, characterized, and implemented. Using the high-impedance property of the offset finite-ground microstrip line, the bandwidth and attenuation depth of the concerned guided-wave bandgap have been quantitatively confirmed to gain the significant enhancement. The two effective per-unit-length parameters were derived in order to display the fundamental guided-wave characteristics of the FGMSL EBG with infinite-extended length [5–7]. The scattering parameters of the finite-cell EBG circuits with varied feed-line impedances were further investigated and found to exhibit bandstop behaviors as a two-port filtering circuit [2–4].

#### REFERENCES

1. R.E. Collin, Foundations for microwave engineering, 2<sup>nd</sup> ed., McGraw-Hill, New York, 1992.
2. F. Yang, R. Coccioli, Y. Qian, and T. Itoh, Planar PBG structures: Basic properties and applications, IEICE Trans Electron E83-C (2000), 687–696.
3. D. Dawn, Y. Ohashi, and T. Shimura, A novel electromagnetic bandgap metal plate for parallel plate mode suppression in shielded structures, IEEE Microwave Wireless Compon Lett 12 (2002), 166–168.
4. R. Abhari and G.V. Eleftheriades, Metallo-dielectric electromagnetic bandgap structures for suppression and isolation of the parallel-plate noise in high-speed circuits, IEEE Trans Microwave Theory Tech 51 (2003), 1629–1639.
5. C.-K. Wu, H.-S. Wu, and C.-K.C. Tzuang, Electric-magnetic-electric slow-wave microstrip line and bandpass filter of compressed size, IEEE Trans Microwave Theory Tech 50 (2002), 1996–2004.
6. S.-G. Mao and M.-Y. Chen, Propagation characteristics of finite-width conductor-backed coplanar waveguides with periodic electromagnetic bandgap cells, IEEE Trans Microwave Theory Tech 50 (2002), 2624–2628.
7. L. Zhu, Guided-wave characteristics of periodic microstrip lines with inductive loading: slow-wave and bandstop behaviors, Microwave Opt Technol Lett (2004), 77–79.
8. S. Sun and L. Zhu, Unified equivalent circuit model of finite-ground microstrip line open-end discontinuities using MoM-SOC technique, IEICE Trans Electron E87-C (2004), 828–831.
9. L. Zhu, Guided-wave characteristics of periodic coplanar waveguides with inductive loading—unit-length transmission parameters, IEEE Trans Microwave Theory Techniques 51 (2003), 2133–2138.

© 2005 Wiley Periodicals, Inc.

## ANTENNA-COUPLED MICROBOLOMETERS ON A SILICON-NITRIDE MEMBRANE

F. J. González,<sup>1</sup> B. Ilic,<sup>2</sup> and G. D. Boreman<sup>3</sup>

<sup>1</sup> Instituto de Investigación en Comunicación Óptica  
Universidad

Autónoma de San Luis Potosí

Alvaro Obregón 64

San Luis Potosí, SLP, México

<sup>2</sup> CNF, Cornell University

Ithaca, NY

<sup>3</sup> UCF, College of Optics & Photonics

Orlando, FL

Received 14 June 2005

**ABSTRACT:** Square-spiral antenna-coupled microbolometers made of gold and chrome are fabricated on a silicon-nitride membrane. The membrane gives mechanical stability and thermal isolation to the detectors so that they can be used as picture elements in commercial infrared-imaging systems. The fabricated devices are measured under room pressure and under vacuum, giving  $D^*$  values of  $3 \times 10^6 \text{ cm}\sqrt{\text{Hz}}/\text{W}$  and  $1.7 \times 10^7 \text{ cm}\sqrt{\text{Hz}}/\text{W}$ , respectively. By using vanadium-oxide, values well above  $1 \times 10^8 \text{ cm}\sqrt{\text{Hz}}/\text{W}$  for  $D^*$  can be obtained. Variations to the fabrication process that will allow the use of vanadium oxide are suggested. © 2005 Wiley Periodicals, Inc. Microwave Opt Technol Lett 47: 246–248, 2005; Published online in Wiley InterScience (www.interscience.wiley.com). DOI 10.1002/mop.21226

**Key words:** antenna-coupled detectors; microbolometers; silicon nitride membrane; responsivity; thermal impedance

#### 1. INTRODUCTION

Antenna-coupled microbolometers have shown response times as low as 130 ns [1] and they can be used as picture elements in infrared-imaging systems [2, 3], which makes them a promising option for fast-frame-rate infrared-imaging applications. The main problem with antenna-coupled microbolometers is that their responsivity is lower than that required for commercial infrared-imaging systems [4].

The responsivity of a microbolometer can be increased by using a bolometric material with a higher temperature coefficient of resistance (TCR) [5] or by increasing the thermal impedance of the device [4]. The highest thermal impedance will occur when the detector is completely isolated from the environment; this will reduce to zero the thermal conductivity of a device. Suspending a device on air above its substrate will increase its thermal impedance by eliminating heat conduction through the substrate [6] (Fig. 1); the standard procedure to make a suspended device is to fabricate it on top of a “sacrificial layer” which will later be selectively etched away, leaving just the patterned structure suspended on air. Silicon dioxide ( $\text{SiO}_2$ ) is widely used as a sacrificial layer because it is easy to deposit and can be etched away with hydrofluoric acid (HF), which will not etch silicon and therefore can be used as an etch-stop.

Thin-film stress and stiction are the main problems associated with fabricating standing structures. Thin-film stress will make the suspended structures buckle and stiction will make the structures collapse due to surface tension of liquids during evaporation; this can be solved by using alternative rinsing procedures such as critical point drying or freeze drying [7].

These problems become important if we increase the area of the suspended devices, which occurs in infrared imaging appli-

cations where a typical pixel covers a  $50 \times 50 \mu\text{m}$  area [3]. Two-dimensional arrays of antenna-coupled microbolometers have been proven to cover typical pixel areas [2], but these structures tend to collapse if they are fabricated as standing structures. Thin-film LPCVD silicon nitride is a very stiff and strong material [8] which has been used as structural material in a great variety of microelectromechanical system (MEMS) devices, such as static membranes, tunable inductors, and tunable MEMS Fabry-Pèrot optical filters [9]. In this paper, an antenna-coupled detector is fabricated on a silicon-nitride ( $\text{Si}_3\text{N}_4$ ) membrane, which will give mechanical stability while maintaining thermal isolation. The procedure shown here can be used to fabricate larger area devices and increase the thermal impedance of 2D arrays of antenna-coupled detectors.

## 2. METHOD

The fabrication procedure consists of thermally growing  $3 \mu\text{m}$  of  $\text{SiO}_2$  on an Si substrate and then growing a 400-nm film of low-stress  $\text{Si}_3\text{N}_4$  using low-pressure chemical-vapor-deposition (LPCVD). A square-spiral-coupled microbolometer was patterned on such a substrate using electron-beam lithography and liftoff via the procedure described in [5]. After the detectors are fabricated, windows are opened near the device on the  $\text{Si}_3\text{N}_4$  film using optical lithography to pattern the windows and reactive ion etching (RIE) to etch away the silicon nitride film, and the  $\text{SiO}_2$  sacrificial layer is etched beneath the  $\text{Si}_3\text{N}_4$  windows using hydrofluoric acid (HF), hence forming a silicon-nitride membrane. Figure 2 shows the formed membrane and the undercut generated with the wet-etching process. Rinsing was performed using a critical point drier (CPD) to avoid stiction. Since HF attacks niobium and other bolometric materials, the antenna-coupled detector was fabricated using gold for the antenna elements and bias line and chrome for the bolometric material (Fig. 2).

## 3. RESULTS

The fabricated devices were placed inside a Dewar vessel and tested using the same procedure described in [3]. The square-spiral detectors on membranes were tested under vacuum and at room pressure. At room pressure, responsivity of 144 V/W and  $D^*$  of  $3 \times 10^6 \text{ cm}\sqrt{\text{Hz}}/\text{W}$  were obtained when the devices were placed under vacuum the responsivity increased to 224 V/W, and  $D^*$

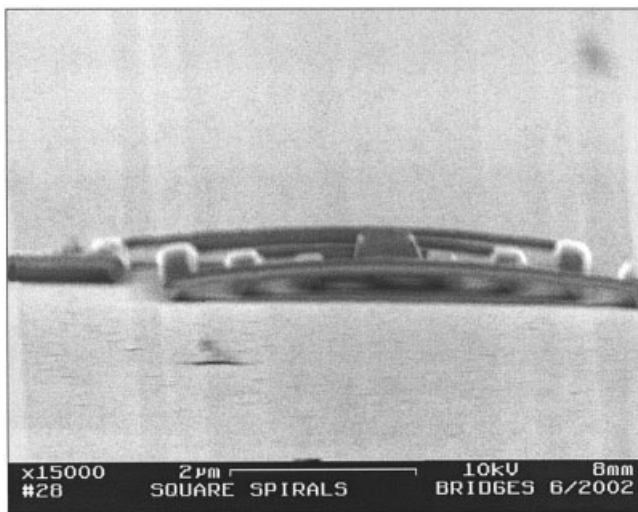


**Figure 1** Suspended square-spiral-coupled microbolometer

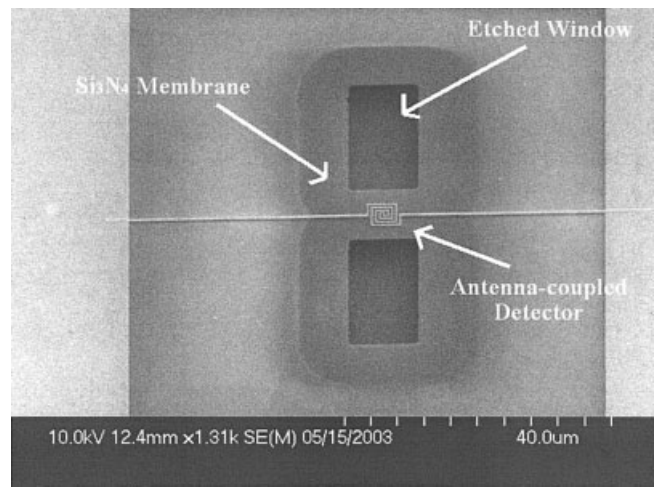


**Figure 2** Square-spiral-coupled microbolometer on a silicon-nitride membrane

showed an even larger increase, given by  $1.7 \times 10^7 \text{ cm}\sqrt{\text{Hz}}/\text{W}$ . Under vacuum the devices showed a smaller noise level, thus giving higher  $D^*$  numbers.

Taking into account that Cr has a TCR  $30\times$  lower than VOx, by fabricating a VOx microbolometer on a membrane values well above  $1 \times 10^3 \text{ V/W}$  and  $1 \times 10^8 \text{ cm}\sqrt{\text{Hz}}/\text{W}$  for responsivity and  $D^*$  should be obtained.

## 4. CONCLUSION

Antenna-coupled detectors have been fabricated on a silicon-nitride membrane, with the membrane providing mechanical stability to the antenna-coupled detectors so that they can be used as picture elements in commercial infrared-imaging systems. The fabricated devices were measured under room pressure and under vacuum, giving  $D^*$  values of  $3 \times 10^6 \text{ cm}\sqrt{\text{Hz}}/\text{W}$  and  $1.7 \times 10^7 \text{ cm}\sqrt{\text{Hz}}/\text{W}$ , respectively.

Even higher responsivity and  $D^*$  values can be obtained if a bolometer with higher TCR is used. The fabrication process can be modified to allow the use of materials that are attacked by HF by masking the devices with chrome [10]. This fabrication procedure will allow the use of materials like titanium, vanadium oxide, and niobium on a silicon-nitride membrane, using silicon dioxide as the sacrificial layer.

## ACKNOWLEDGMENTS

This work was performed in part at the Cornell Nanofabrication Facility (a member of the National Nanofabrication Users Network) which is supported by the National Science Foundation under grant no. ECS-9731293, its users, Cornell University, and Industrial Affiliates. F. J. González acknowledges the support of SEP and UASLP-FAI through grant nos. PROMEP/103.5/04/1386 and C04-FAI-04-11.13, respectively.

## REFERENCES

1. F.J. González, C. Fumeaux, J. Alda, and G.D. Boreman, Thermal impedance model of electrostatic discharge effects on microbolometers, *Microwave Opt Technol Lett* 26 (2000), 291–293.
2. F.J. González, M.A. Gritz, C. Fumeaux, and G.D. Boreman, Two-dimensional array of antenna-coupled detectors, *Int J Infrared Millimeter Waves* 23 (2002), 785–797.
3. F.J. González, B. Ilic, J. Alda, and G.D. Boreman, Antenna-coupled

- infrared detectors for imaging applications, IEEE JSTQE 11 (2005), 117–120.
4. F.J. González, C.S. Ashley, P.G. Clem, and G.D. Boreman, Antenna-coupled microbolometer arrays with aerogel thermal isolation, *Infrared Phys Tech* 45 (2004), 47–51.
  5. F.J. González, M. Abdel-Rahman, and G.D. Boreman, Antenna-coupled VOx thin-film microbolometer array, *Microwave Opt Technol Lett* 38 (2003), 235–237.
  6. D.P. Neikirk and D.B. Rutledge, Air-bridge microbolometer for far infrared detection, *Appl Phys Lett* 44 (1984), 153–155.
  7. M. Elwenspoek, and R. Wiegerink, *Mechanical Microsensors*, Springer-Verlag, 2001.
  8. R.L. Edwards, G. Coles, and W.N. Sharpe, Jr., Comparison of tensile and bulge tests for thin-film silicon nitride, *Experimen Mechan* 44 (2004), 49–54.
  9. H. Huang, K. Winchester, Y. Liu, X.Z. Hu, C.A. Musca, J.M. Dell, and L. Faraone, Determination of mechanical properties of PECVD silicon nitride thin films for tunable MEMS Fabry-Pérot optical filters, *J Micromech Microeng* 15 (2005), 608–614.
  10. M.A. Gritz, I. Puscasu, D. Spencer, et al., Fabrication of an infrared antenna-coupled microbolometer linear array using chrome as a mask, *JVST B* 21 (2003), 2608–2611.

© 2005 Wiley Periodicals, Inc.

## EXTENSION OF THE ANALYTICAL MODELLING OF RESISTIVE LOADED THIN-WIRE ANTENNAS TO GAUSSIAN DERIVATIVES EXCITATIONS

F. Sagnard<sup>1,2</sup> and C. Vignat<sup>2</sup>

<sup>1</sup> IETR, UMR 6164, INSA  
20, avenue des Buttes de Coësmes  
35043 Rennes, France

<sup>2</sup> IGM, Université de Marne-La-Vallée  
77454 Marne-La-Vallée cedex 2, France

Received 10 June 2005

**ABSTRACT:** *The transient electric field radiated from a thin-wire dipole antenna resistively loaded and excited by a voltage signal in the shape of the Gaussian derivatives is analyzed. The modelling presented in this paper is formulated in the time domain using an inverse Fourier transform of the analytical expressions obtained by Wu and King in the frequency domain. Such a modelling appears as an extension of previous developments, as it allows us to consider any Gaussian derivatives as excitation signals as well as the presence of a nonnegligible impedance in the feeding circuit. Parameter studies are presented to analyze the waveforms and the energy radiated in the far-field zone.* © 2005 Wiley Periodicals, Inc. *Microwave Opt Technol Lett* 47: 548–553, 2005; Published online in Wiley InterScience (www.interscience.wiley.com). DOI 10.1002/mop.21227

**Key words:** *broadband antenna; Gaussian excitation; thin-wire antenna; transient response; electromagnetic radiation*

### 1. INTRODUCTION

Wireless data transmission at high rate, short range, and low cost appears to be an alternative for numerous applications dealing with communications, networking, radar, imaging, and positioning systems. Ultra-wideband (UWB) technology provides significant potential, as it relies on the radiation and propagation of extremely large baseband pulses characterized by a spectral occupancy in excess of 500 MHz and a fractional bandwidth of more than 20% [1]. As this technology aims to maximize the utilization of underused spectrum segments with-

out licence, and to minimize interference with other communication systems, the maximum allowable power spectral density (PSD) should be specified. Thus, in February 2002, the FCC defined a spectral mask, and the ETSI is currently working on a similar mask which appears to be more restrictive. For the design and evaluation of an UWB communication link, critical points are evaluation of the energy loss and the waveform distortions experienced by the transmitted signal which has propagated through a multipath channel [2].

In fact, the transmitting and receiving antennas appear to influence the overall performances of UWB systems significantly. In particular, the UWB transmitter and receiver should ideally have flat responses and linear phase variations versus frequency over the frequency band of interest. Deviations from these constraints will cause distortion in the initial signal. In this paper, we focus our studies on the transient waveforms radiated in the transmission configuration by thin-wire antennas when they are excited by a short transient signal generated by a voltage source. The voltage signal is assumed to have the shape of the Gaussian function or one of its successive derivatives. To correlate and analyze the waveforms radiated with the physical phenomena involved, we consider the basic dipole antenna because it can be described using analytical relations. Moreover, such an antenna allows us to consider an assembly of thin-wire elements in order to present approximated models of antennas such as the V-dipole, the bow-tie antenna, and the TEM hornlike antenna. The dipoles studied include a passive load to prevent reflection at the top end in order to satisfy broadband characteristics. Such a behaviour can be obtained by different means; the loading technique proposed by Wu and King in 1965, which considers a distributed resistive profile along the antenna, has been found to be very efficient [3]. The time-domain modelling proposed in this paper appears as an extension of previous studies, as it allows us to consider all voltage excitations which have the shape of the Gaussian function and its successive derivatives. Moreover, an equivalent impedance associated with the input circuit has been included in the modelling. The electric-field waveforms radiated are calculated and analyzed in the far-field zone. The parametric studies presented demonstrate the influence, on the waveforms and the energy radiated, of the duration and the shape of the incident pulse, the source impedance, and the antenna geometry. Such studies form an aid to improve the physical phenomena involved in the transient radiation of more complex ultra-wideband antennas.

### 2. TRANSIENT RESPONSE OF A DIPOLE ANTENNA

#### 2.1. General Principles

The dipole antenna is made of two finite-length thin cylinders (or arms) of length  $L$ ; it is assumed to be initially centred and aligned with the  $Oz$  axis so that the feed point is positioned at  $z = 0$ . It is included in an electric circuit, as shown in Figure 1. A voltage generator  $V_g$  is supposed to deliver an excitation signal in the equivalent circuit made of three impedances: the source impedance ( $Z_g$ ), the impedance of the transmission line linking the generator to the antenna feed-point ( $Z_l$ ), and the input antenna impedance at the feed-point  $Z_A$  [4]. In general, all these impedances depend on frequency. In the circuit, the presence of nonuniform impedances and impedance mismatches over the frequency bandwidth of the excitation signal causes signal distortions. In the frequency domain, the relation between the input voltage and the resulting current is given by